JOURNAL OF GUIDANCE, CONTROL, AND DYNAMICS
Vol. 37, No. 6, pp. 2030–2035.

Engineering Notes

Shadow Set Considerations for Modified Rodrigues Parameter Attitude Filtering

Stephen A. O'Keefe* and Hanspeter Schaub†
University of Colorado, Boulder, Colorado 80309

DOI: 10.2514/1.G000405

I. Introduction

RIGID-BODY attitude estimation algorithms have been previously formulated using modified Rodrigues parameter (MRP) attitude sets. These MRP-based attitude estimation algorithms are attractive because they have been shown to have equal accuracy to and faster initial convergence than similar quaternion-based filters, and they avoid the quaternion constraint problem [1]. These algorithms make use of the fact that two MRP sets describe a particular orientation and singularity avoidance is performed by switching between the original MRP set and the alternate set, known as the shadow set. Unfortunately, the nonuniqueness of MRPs can lead to significant attitude estimation errors through improper calculation of the measurement residual. This work examines the handling of measurement residuals within existing MRP attitude estimators, specifically the technical details of when and how to switch to and from the MRP shadow set when calculating the measurement residual.

Attitude estimation is often performed using an extended Kalman filter (EKF) with quaternions as the attitude measure [2,3]. Quaternions lend themselves well to attitude estimation because they represent a redundant, nonsingular attitude description with globally nonsingular kinematics, elegant successive rotation expressions, and rigorously linear kinematic differential equations. However, the quaternion unit norm constraint complicates matters and has led to extended discussions of attitude estimation and constraints [4–6].

Other attitude parameterizations can be used in filtering, assuming that appropriate strategies are employed to avoid singularities; examples include Euler angles [7,8], classical Rodrigues parameters [9], and MRPs. MRPs are of particular interest because they are a minimal three-parameter attitude set that are nonsingular for any rotation other than multiples of 2π. Schaub and Junkins [10] note that two MRP sets exist to describe a particular orientation, and the second set, known as the shadow set, is nonsingular for nonzero rotations. Therefore, singularity avoidance is performed by switching between the two sets. Further, both sets obey the same differential equations, making for easy implementation.

MRPs, first explored as an attitude estimation parameterization in 1996 [11] and discussed in detail in [10], have been used to develop globally stabilizing feedback control [12], optimal attitude control [13], and sliding mode control for maneuvers [14]. Lee and Alfriend present an additive divided difference filter using MRPs, but do not discuss the transformation of the covariance when switching to the shadow MRP set [15]. Cheng and Crassidis propose using MRPs in a particle filter and they mention that MRP switching may cause discontinuities of the covariance, but do not provide an appropriate covariance mapping‡ [16]. Jizheng et al. also note that the covariance experiences a discontinuity at the point where the MRP is switched and propose a first-order covariance mapping [17]. Karlgaard and Schaub provide a first-order covariance mapping for use in an additive MRP EKF, and additionally provide first- and second-order transformations suitable for use in divided difference filters [1]. Furthermore, they show an additive MRP EKF to have equal accuracy to and faster initial convergence than quaternion filters with slightly faster numerical evaluation and vastly simpler coding implementation. Unfortunately, none of the previously published MRP EKF implementations address the issues that arise when dealing with observations.

The present work examines the details required for proper calculation of observation residuals within existing MRP EKF formulations. Specifically, this paper covers a novel method for determining when and how to switch to and from the MRP shadow set when calculating the measurement residual. A brief overview of the relevant aspects of modified Rodrigues parameters is presented first. Next, the derivation of an additive MRP EKF, complete with an appropriate first-order analytical covariance mapping to be used when switching the MRPs to or from their shadow set, is reviewed. This additive MRP EKF is then used to illustrate the issues corresponding to the calculation of the measurement residual that can arise due to the nonuniqueness of MRPs, and a method for mitigating these issues is discussed. Finally, numerical simulation results demonstrating these issues and the performance of the mitigation algorithms are presented.

II. Modified Rodrigues Parameters

The modified Rodrigues parameter vector $\boldsymbol{\sigma}$ is defined in terms of the principal rotation elements as

$$\boldsymbol{\sigma} = \hat{\boldsymbol{e}} \tan\left(\frac{\Phi}{4}\right) \tag{1}$$

where $\hat{\boldsymbol{e}}$ is the principal rotation axis, and Φ is the principal rotation angle [10,18]. The MRP shadow set is defined as

$$\boldsymbol{\sigma}^S = -\frac{\boldsymbol{\sigma}}{\boldsymbol{\sigma}^T\boldsymbol{\sigma}} \tag{2}$$

and both MRPs satisfy the differential equation

$$\dot{\boldsymbol{\sigma}} = \frac{1}{4}[(1-\boldsymbol{\sigma}^T\boldsymbol{\sigma})[\boldsymbol{I}_{3\times3}] + 2[\boldsymbol{\sigma}]_\times + 2\boldsymbol{\sigma}\boldsymbol{\sigma}^T]\boldsymbol{\omega} = \frac{1}{4}[B(\boldsymbol{\sigma})]\boldsymbol{\omega} \tag{3}$$

where $[\cdot]_\times$ represents the skew-symmetric cross product matrix given by

$$[\boldsymbol{\sigma}]_\times = \begin{bmatrix} 0 & -\sigma_3 & \sigma_2 \\ \sigma_3 & 0 & -\sigma_1 \\ -\sigma_2 & \sigma_1 & 0 \end{bmatrix}$$

The inverse MRP is given by $\boldsymbol{\sigma}^{-1} \equiv -\boldsymbol{\sigma}$ and the successive rotation of two MRPs is computed using the MRP product

Presented as Paper 2013-889 at the AAS/AIAA Astrodynamics Specialist Conference, Hilton Head, SC, 11–15 August 2013; received 24 November 2013; revision received 8 January 2014; accepted for publication 14 January 2014; published online 28 April 2014.

*Graduate Student, Aerospace Engineering Sciences.
†Professor, Aerospace Engineering Sciences. Associate Fellow AIAA.

‡Covariance mapping is not actually required in their particle filtering approach.

$$\bar{\bar{\boldsymbol{\sigma}}} = \bar{\boldsymbol{\sigma}} \otimes \boldsymbol{\sigma} = \frac{(1 - \boldsymbol{\sigma}^T\boldsymbol{\sigma})\bar{\boldsymbol{\sigma}} + (1 - \bar{\boldsymbol{\sigma}}^T\bar{\boldsymbol{\sigma}})\boldsymbol{\sigma} - 2[\bar{\boldsymbol{\sigma}}]_\times\boldsymbol{\sigma}}{1 + (\boldsymbol{\sigma}^T\boldsymbol{\sigma})(\bar{\boldsymbol{\sigma}}^T\bar{\boldsymbol{\sigma}}) - 2\bar{\boldsymbol{\sigma}}^T\boldsymbol{\sigma}} \tag{4}$$

For more information regarding MRPs, the reader is referred to [10].

III. MRP Kalman Filter Formulation

A common spacecraft attitude estimation problem involves propagating state dynamics using an inertial angular velocity vector, sensed via a rate gyroscope, and correcting that estimate using a direct measurement of the body's attitude, via a star tracker or other generic attitude sensor [2,3,19]. An additive MRP EKF approach, as proposed by Karlgaard and Schaub [1], is used here to illustrate the issues that can arise when computing the observation residual, but it is important to note that the same issues arise with a multiplicative attitude estimation approach.

The MRP EKF assumes the gyroscope dynamics follow Farrenkopf's approximation [20]

$$\boldsymbol{\omega} = \tilde{\boldsymbol{\omega}} - \boldsymbol{\omega}_b - \boldsymbol{\eta}_\omega \tag{5}$$

$$\dot{\boldsymbol{\omega}}_b = \boldsymbol{\eta}_{\omega_b} \tag{6}$$

where $\tilde{\boldsymbol{\omega}}$ represents the sensed angular velocity, $\boldsymbol{\omega}$ is the true angular velocity, $\boldsymbol{\omega}_b$ is the measurement bias, and $\boldsymbol{\eta}_\omega$ and $\boldsymbol{\eta}_{\omega_b}$ are zero-mean Gaussian white-noise processes with spectral densities given by $\boldsymbol{\sigma}_\omega^2 \boldsymbol{I}_{3\times3}$ and $\boldsymbol{\sigma}_{\omega_b}^2 \boldsymbol{I}_{3\times3}$, respectively. It follows that the state dynamics are given by

$$\dot{\boldsymbol{x}} = \boldsymbol{f}(\boldsymbol{x}) + \boldsymbol{g}(\boldsymbol{x}, \boldsymbol{\eta}) \tag{7}$$

where $\boldsymbol{x} = [\boldsymbol{\sigma}, \boldsymbol{\omega}_b]^T$, $\boldsymbol{\eta} = [\boldsymbol{\eta}_\omega, \boldsymbol{\eta}_{\omega_b}]^T$, and

$$\boldsymbol{f}(\boldsymbol{x}) = \begin{bmatrix} \frac{1}{4}[B(\boldsymbol{\sigma})](\tilde{\boldsymbol{\omega}} - \boldsymbol{\omega}_b) \\ 0_{3\times3} \end{bmatrix} \tag{8}$$

$$\boldsymbol{g}(\boldsymbol{x}, \boldsymbol{\eta}) = \begin{bmatrix} -\frac{1}{4}[B(\boldsymbol{\sigma})]\boldsymbol{\eta}_\omega \\ \boldsymbol{\eta}_{\omega_b} \end{bmatrix} \tag{9}$$

Thus, continuous-time propagation of the state and covariance is performed by numerically integrating Eq. (7) and the Lyapunov differential equation [21]

$$\dot{\hat{\boldsymbol{P}}} = \boldsymbol{F}\hat{\boldsymbol{P}} + \hat{\boldsymbol{P}}\boldsymbol{F}^T + \boldsymbol{G}\boldsymbol{Q}\boldsymbol{G}^T \tag{10}$$

where $\hat{\boldsymbol{P}}$ represents the current estimate of the state covariance, and

$$\boldsymbol{F} \equiv \left.\frac{\partial \boldsymbol{f}}{\partial \boldsymbol{x}}\right|_{x=\hat{x}} = \begin{bmatrix} \frac{1}{2}(\hat{\boldsymbol{\sigma}}\hat{\boldsymbol{\omega}}^T - \hat{\boldsymbol{\omega}}\hat{\boldsymbol{\sigma}}^T - [\hat{\boldsymbol{\omega}}]_\times + \hat{\boldsymbol{\sigma}}^T\hat{\boldsymbol{\omega}}\boldsymbol{I}) & -\frac{1}{4}[B(\hat{\boldsymbol{\sigma}})] \\ 0_{3\times3} & 0_{3\times3} \end{bmatrix} \tag{11}$$

$$\boldsymbol{G} \equiv \left.\frac{\partial \boldsymbol{g}}{\partial \boldsymbol{\eta}}\right|_{x=\hat{x},\boldsymbol{\eta}=0} = \begin{bmatrix} -\frac{1}{4}[B(\hat{\boldsymbol{\sigma}})] & 0_{3\times3} \\ 0_{3\times3} & \boldsymbol{I}_{3\times3} \end{bmatrix} \tag{12}$$

where $\hat{\boldsymbol{\sigma}}$ and $\hat{\boldsymbol{\omega}}_b$ are the best estimates of the attitude MRP and rate gyroscope bias, respectively, output by the EKF and $\hat{\boldsymbol{\omega}} = \tilde{\boldsymbol{\omega}} - \hat{\boldsymbol{\omega}}_b$.

The attitude sensing device measurements are assumed to take the form

$$\tilde{\boldsymbol{\sigma}} = \boldsymbol{\sigma} \otimes \delta\boldsymbol{\sigma} \tag{13}$$

where $\tilde{\boldsymbol{\sigma}}$ represents the measured MRP, $\boldsymbol{\sigma}$ represents the true attitude, and $\delta\boldsymbol{\sigma}$ represents an attitude measurement error. It is assumed that all measurements $\tilde{\boldsymbol{\sigma}}$ are given by the MRP representation corresponding to a principle rotation angle less than 180 deg, thus the magnitude of the reported measurement MRP will always be less than one. Using the measurement equation

$$\boldsymbol{h}(\boldsymbol{x}) = \hat{\boldsymbol{\sigma}} \tag{14}$$

discrete-time measurements at time t_k are incorporated into the propagated state $\hat{\boldsymbol{x}}_k^-$ and covariance $\hat{\boldsymbol{P}}_k^-$ estimates to give an updated state $\hat{\boldsymbol{x}}_k^+$ and covariance $\boldsymbol{P}_k^+$ estimate using

$$\hat{\boldsymbol{x}}_k^+ = \hat{\boldsymbol{x}}_k^- + \boldsymbol{K}_k\boldsymbol{y}_k \tag{15}$$

$$\hat{\boldsymbol{P}}_k^+ = [\boldsymbol{I} - \boldsymbol{K}_k\boldsymbol{H}_k(\hat{\boldsymbol{x}}_k^-)]\hat{\boldsymbol{P}}_k^-[\boldsymbol{I} - \boldsymbol{K}_k\boldsymbol{H}_k(\hat{\boldsymbol{x}}_k^-)]^T + \boldsymbol{K}_k\boldsymbol{R}_k\boldsymbol{K}_k^T \tag{16}$$

where the measurement residual is given by $\boldsymbol{y}_k = \tilde{\boldsymbol{\sigma}}_k - \hat{\boldsymbol{\sigma}}_k$. The Kalman gain $\boldsymbol{K}_k$ at time t_k is given by

$$\boldsymbol{K}_k = \hat{\boldsymbol{P}}_k^-\boldsymbol{H}_k^T(\hat{\boldsymbol{x}}_k^-)[\boldsymbol{H}_k(\hat{\boldsymbol{x}}_k^-)\hat{\boldsymbol{P}}_k^-\boldsymbol{H}_k^T(\hat{\boldsymbol{x}}_k^-) + \boldsymbol{R}_k]^{-1} \tag{17}$$

where

$$\boldsymbol{H}_k(\hat{\boldsymbol{x}}_k^-) \equiv \left.\frac{\partial \boldsymbol{h}}{\partial \boldsymbol{x}}\right|_{\hat{x}_k^-} = [\,\boldsymbol{I}_{3\times3} \quad 0_{3\times3}\,] \tag{18}$$

If, after propagating, using Eq. (7), or performing an update, using Eqs. (15) and (16), the estimated MRP's magnitude is greater than one $\|\hat{\boldsymbol{\sigma}}_k\| > 1$, the MRP attitude set is switched to the shadow set. The shadow set transformation of the state vector is given by

$$\boldsymbol{x}^S = \begin{bmatrix} -(\boldsymbol{\sigma}^T\boldsymbol{\sigma})^{-1}\boldsymbol{\sigma} \\ \boldsymbol{\omega}_b \end{bmatrix} \tag{19}$$

The shadow set transformation of the covariance matrix is found by decomposing the covariance matrix into submatrices

$$\boldsymbol{P} = \begin{bmatrix} \boldsymbol{P}_{\sigma\sigma} & \boldsymbol{P}_{\sigma\omega_b} \\ \boldsymbol{P}_{\sigma\omega_b}^T & \boldsymbol{P}_{\omega_b\omega_b} \end{bmatrix}$$

where $\boldsymbol{P}_{xx}$ is the covariance matrix of x, and $\boldsymbol{P}_{xy}$ is the cross-correlation matrix between x and y. The mapping of the covariance matrix to the shadow set is given by [1]

$$\boldsymbol{P}^S = \begin{bmatrix} \boldsymbol{S}\boldsymbol{P}_{\sigma\sigma}\boldsymbol{S}^T & \boldsymbol{S}\boldsymbol{P}_{\sigma\omega_b} \\ \mathcal{P}_{\sigma\omega_b}^T\boldsymbol{S}^T & \boldsymbol{P}_{\omega_b\omega_b} \end{bmatrix} \tag{20}$$

where

$$\boldsymbol{S} = 2\sigma^{-4}\boldsymbol{\sigma}\boldsymbol{\sigma}^T - \sigma^{-2}\boldsymbol{I}_{3\times3}$$

and $\sigma^2 = \boldsymbol{\sigma}^T\boldsymbol{\sigma}$.

Although an additive approach to an MRP EKF is presented here, it is important to note that a multiplicative MRP EKF is also viable and provides similar estimation accuracy. Such a filter uses a true relative orientation residual as opposed to the numerical residual used in Eq. (16) and is derived by following the multiplicative quaternion EKF formulation in [19].

IV. MRP Shadow Set Considerations

Of particular interest here is the computation of the measurement residual $\boldsymbol{y}_k$, the difference between the measured $\tilde{\boldsymbol{\sigma}}_k$ and estimated attitude $\hat{\boldsymbol{\sigma}}_k$ at time t_k, which has not previously been discussed in detail. For the additive MRP EKF, the measurement residual is given by the numerical difference

$$\boldsymbol{y}_k = \tilde{\boldsymbol{\sigma}}_k - \hat{\boldsymbol{\sigma}}_k \tag{21}$$

As discussed earlier, due to the nonuniqueness of MRPs, there are always two MRP sets to describe the same orientation. This can become an issue if the magnitude of the discrete MRP measurement $\|\tilde{\boldsymbol{\sigma}}_k\|$ or estimate $\|\hat{\boldsymbol{\sigma}}_k\|$ is near one. For example, if $\tilde{\boldsymbol{\sigma}}_k = [1, 0, 0]$ and $\hat{\boldsymbol{\sigma}}_k = [-1, 0, 0]$, which represents the same physical orientation as $\tilde{\boldsymbol{\sigma}}_k^S$,

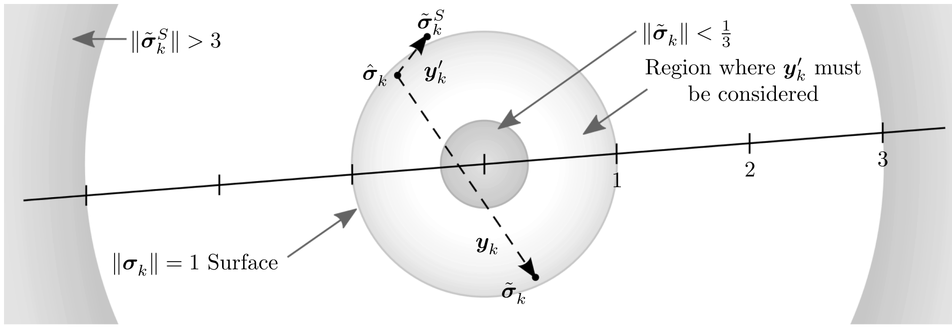

Fig. 1 Illustration of possible measurement residual at a specific time and region where y_k' must be considered.

both values describe the same attitude and thus the measurement residual should be $[0, 0, 0]$. However, Eq. (21) will result in a measurement residual of $[2, 0, 0]$ and the update equation given by Eq. (15) will apply a correction when none is needed, thus degrading the estimate of the attitude.

To avoid this issue in practice, a new approach is proposed in which the measurement residual is calculated a second time using

$$\boldsymbol{y}_k' = \tilde{\boldsymbol{\sigma}}_k^S - \hat{\boldsymbol{\sigma}}_k \tag{22}$$

where $\tilde{\boldsymbol{\sigma}}_k^S$ is evaluated using Eq. (2). The quantity $\boldsymbol{y}_k$ or $\boldsymbol{y}_k'$ with the smaller magnitude is then used in Eq. (15) and estimation continues. Figure 1 illustrates graphically the situation where $\|\boldsymbol{y}_k'\| < \|\boldsymbol{y}_k\|$ and Algorithm 1 provides pseudocode for the proposed algorithm. Note that, although the measurements $\tilde{\boldsymbol{\sigma}}$ are assumed to be noisy, the measurement at t_k is a discrete value and $\|\tilde{\boldsymbol{\sigma}}_k\|$ is the magnitude of this discrete value.

Performing this additional calculation at every time step does not represent a significant computational burden, however, an issue does develop when a measurement has a magnitude near zero. When $\|\tilde{\boldsymbol{\sigma}}_k\| \to 0$ the shadow set $\|\tilde{\boldsymbol{\sigma}}_k^S\| \to \infty$ and is ill defined. In this scenario, the magnitude of the original measured MRP $\|\tilde{\boldsymbol{\sigma}}_k\|$ is always less than the magnitude of the shadow MRP set of the measurement $\|\tilde{\boldsymbol{\sigma}}_k^S\|$ and there is no need to evaluate Eq. (22). For this reason, a bound is placed on when to evaluate Eq. (22). As noted earlier, both $\tilde{\boldsymbol{\sigma}}_k$ and $\hat{\boldsymbol{\sigma}}_k$ are assumed to be constrained with a magnitude less than or equal to one, which implies, at any time t_k,

$$\|\boldsymbol{y}_k\| \leq 2$$

Therefore, conservatively, if the magnitude of the measured MRP's shadow set $\tilde{\boldsymbol{\sigma}}_k^S$ at time t_k is greater than three, the magnitude of $\boldsymbol{y}_k'$ must be greater than $\boldsymbol{y}_k$

$$\|\tilde{\boldsymbol{\sigma}}_k^S\| > 3 \Rightarrow \|\boldsymbol{y}_k\| < \|\boldsymbol{y}_k'\|$$

and $\boldsymbol{y}_k'$ need not be calculated. By applying Eq. (2), it is evident that

$$\|\tilde{\boldsymbol{\sigma}}_k^S\| > 3 \Rightarrow \|\tilde{\boldsymbol{\sigma}}_k\| < 1/3$$

Thus, a conservative bound on when the calculation of $\boldsymbol{y}_k'$ can be ignored is when $\|\tilde{\boldsymbol{\sigma}}_k\| < 1/3$. Therefore, when $1/3 < \|\tilde{\boldsymbol{\sigma}}_k\| < 1$, as illustrated in Fig. 1, the check described earlier should be computed.

Algorithm 1 Proposed measurement residual algorithm for additive MRP EKF

$\boldsymbol{y}_k = \tilde{\boldsymbol{\sigma}}_k - \hat{\boldsymbol{\sigma}}_k$
if $\|\tilde{\boldsymbol{\sigma}}_k\| > \frac{1}{3}$ **then**
  $\boldsymbol{y}_k' = \tilde{\boldsymbol{\sigma}}_k^S - \hat{\boldsymbol{\sigma}}_k$
  if $\|\boldsymbol{y}_k'\| < \|\boldsymbol{y}_k\|$ **then**
    $\boldsymbol{y}_k = \boldsymbol{y}_k'$
  end if
end if

For a multiplicative MRP EKF, the measurement residual at time t_k is given by the relative orientation difference

$$\boldsymbol{y}_k = \tilde{\boldsymbol{\sigma}}_k \otimes \hat{\boldsymbol{\sigma}}_k^{-1} \tag{23}$$

Using the example provided earlier, where $\tilde{\boldsymbol{\sigma}} = [1, 0, 0]$ and $\hat{\boldsymbol{\sigma}} = [-1, 0, 0]$, evaluating Eq. (23) results in a division by zero and, in other cases, can lead to an erroneously large residual when the resulting MRP describes a rotation with a principal rotation angle greater than 180 deg. To avoid this, a similar approach is proposed where the measurement residual is calculated a second time using the shadow set of the measurement

$$y_k' = \tilde{\boldsymbol{\sigma}}_k^S \otimes \hat{\boldsymbol{\sigma}}_k^{-1} \tag{24}$$

and the quantity $\boldsymbol{y}_k$ or $\boldsymbol{y}_k'$ with the smaller magnitude is used in the update equations. Algorithm 2 provides pseudocode for a multiplicative MRP EKF. In this case, $\|\tilde{\boldsymbol{\sigma}}_k\|$ is compared with a sufficiently small number ϵ to prevent division by zero.

As an alternative, Eq. (23) could be calculated using direction cosine matrices

$$[C(\boldsymbol{y}_k)] = [C(\tilde{\boldsymbol{\sigma}}_k)][C(-\hat{\boldsymbol{\sigma}}_k)]$$

and extracting the resultant MRP set with the smaller principal rotation angle, but this is found in practice to be significantly more computationally demanding than the proposed algorithm.

V. Results

A simple numerical simulation is presented to illustrate the performance of the nonsingular additive MRP EKF and highlight certain implementation details. The uncontrolled tumbling motion of a small spacecraft is modeled assuming the spacecraft has principle inertia values of $I_1 = 4$, $I_2 = 4$, and $I_3 = 3\ \mathrm{kg \cdot m^2}$. The initial attitude of the spacecraft is given by $\boldsymbol{\sigma}(t_0) = [0.3, 0.1, -0.5]^T$. The initial angular velocity is given by $\boldsymbol{\omega}(t_0) = [-0.2, 0.2, -0.1]^T$ deg/s.

Attitude measurements are simulated at 0.2 Hz with an attitude measurement error covariance of 20 arcsec. The measurement covariance for the additive filter is set to $\boldsymbol{R} = 0.0004\boldsymbol{I}_{3\times3}$. The

Algorithm 2 Proposed measurement residual algorithm for multiplicative MRP EKF

$\boldsymbol{y}_k = \tilde{\boldsymbol{\sigma}}_k \otimes \hat{\boldsymbol{\sigma}}_k^{-1}$
if $\|\tilde{\boldsymbol{\sigma}}_k\| > \epsilon$ **then**
  $\boldsymbol{y}_k' = \tilde{\boldsymbol{\sigma}}_k^S \otimes \hat{\boldsymbol{\sigma}}_k^{-1}$
  if $\|\boldsymbol{y}_k'\| < \|\boldsymbol{y}_k\|$ **then**
    $\boldsymbol{y}_k = \boldsymbol{y}_k'$
  end if
end if

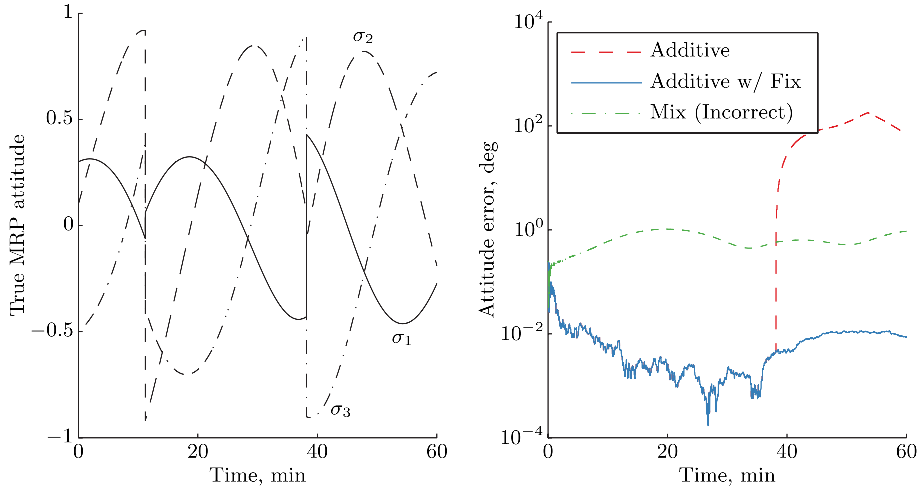

a) True spacecraft attitude b) Attitude estimate error

Fig. 2 Results of simulation using additive MRP EKF with and without proposed algorithm illustrating importance.

angular rate measurements are simulated at 2.0 Hz, assuming an initial bias of $\boldsymbol{\omega}_{b_0} = [-1.0, 2.0, -3.0]^T$ deg /h and $\sigma_\omega = \sqrt{10} \times 10^{-7}$ rad/s$^{1/2}$ and $\sigma_{\omega_b} = \sqrt{10} \times 10^{-10}$ rad/s$^{3/2}$. The initial attitude estimate is $\hat{\boldsymbol{\sigma}} = 0_{3\times1}$ and the initial angular rate bias estimate is $\hat{\boldsymbol{\omega}}_b = 0_{3\times1}$. The initial covariance matrix is given by $\hat{\boldsymbol{P}}_0 = \text{diag}[P_\sigma, P_\sigma, P_\sigma, P_{\omega_b}, P_{\omega_b}, P_{\omega_b}]$ where $P_\sigma = 0.175$ rad^2 and $P_{\omega_b} = 0.005$ rad^2/s^2.

The time history of the true attitude and the principal rotation error of the estimate for a 60 min simulation are shown in Fig. 2. It can be seen that not all instances of MRP switching require the proposed algorithm, for instance, the estimator handles the switching at 11.2 min quite well. An example of when $\|\boldsymbol{y}_k'\| < \|\boldsymbol{y}_k\|$ is seen at 38.2 min. At that time, simply calculating the vector difference between $\tilde{\boldsymbol{\sigma}}_k$ and $\hat{\boldsymbol{\sigma}}_k$ results in

$$\boldsymbol{y}_k = [0.859201 \quad -0.137457 \quad -1.800605]$$

whereas using the shadow MRP set of the measurement results in

$$\boldsymbol{y}_k' = [-0.000006 \quad -0.000048 \quad 0.000195]$$

Clearly, $\boldsymbol{y}_k$ represents a spuriously large error in the attitude estimate and the original additive estimator diverges, whereas by using the shadow MRP set of the measured attitude, the magnitude of the measurement residual is very close to zero.

It is important when using an additive filter to use a numerical difference for the measurement residual and when using a multiplicative filter to use a multiplicative residual. Included in Fig. 2b are the results for an additive filter using a multiplicative residual, illustrating the poor performance resulting from such an incorrect mixture of methods.

The state estimates and their associated covariance bounds for the proposed algorithm are shown in Fig. 3. Both the attitude MRP and rate gyroscope bias estimates can be seen to quickly converge to the noise level while remaining within the 1σ covariance bounds, despite the relatively slow attitude measurement update rate.

VI. Conclusions

The details associated with calculating the measurement residual, specifically switching to and from the MRP shadow set, for an MRP EKF performing attitude estimation are discussed. It is shown analytically and with numerical simulation that, when calculating the measurement residual, it is important that there are two valid MRP representations for any one attitude. Calculating the measurement residual using the attitude measurement MRP shadow set does not represent a significant computational burden; however, issues arise when $\|\tilde{\boldsymbol{\sigma}}_k\| \to 0$. A conservative bound of $\|\tilde{\boldsymbol{\sigma}}_k\| < 1/3$ has been established for when to calculate the measurement residual using the shadow set of the measurement MRP when using an additive MRP EKF. The MRP EKF provides a globally nonsingular attitude estimation algorithm with a minimal attitude representation, but care

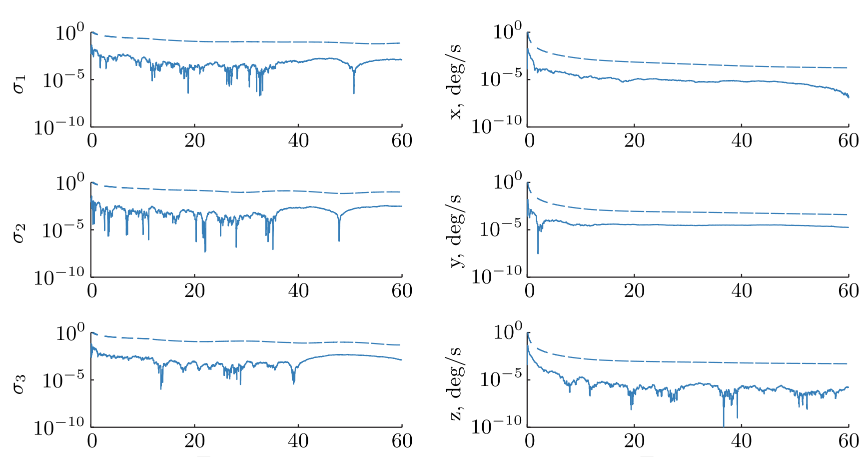

a) $\boldsymbol{\sigma}$ estimate errors b) $\boldsymbol{\omega}_b$ estimate errors

Fig. 3 Results of numerical simulation using proposed method showing convergence of all states. Dotted lines indicate 1σ covariance bounds.

must be taken when switching attitude estimate to and from the MRP shadow set.

References

[1] Karlgaard, C. D., and Schaub, H., "Nonsingular Attitude Filtering Using Modified Rodrigues Parameters," *Journal of Astronautical Sciences*, Vol. 57, No. 4, 2010, pp. 777–791.

[2] Lefferts, E. J., Markley, F. L., and Shuster, M. D., "Kalman Filtering for Spacecraft Attitude Estimation," *Journal of Guidance, Control, and Dynamics*, Vol. 5, No. 5, 1982, pp. 417–429. doi:10.2514/3.56190

[3] Crassidis, J. L., Markley, F. L., and Cheng, Y., "Survey of Nonlinear Attitude Estimation Methods," *Journal of Guidance, Control, and Dynamics*, Vol. 30, No. 1, 2007, pp. 12–28. doi:10.2514/1.22452

[4] Shuster, M. D., "Constraint in Attitude Estimation Part I: Constrained Estimation 1," *Journal of Astronautical Sciences*, Vol. 51, No. 1, 2003, pp. 51–74.

[5] Shuster, M. D., "Constraint in Attitude Estimation Part II: Unconstrained Estimation 1," *Journal of Astronautical Sciences*, Vol. 51, No. 1, 2003, pp. 75–101.

[6] Markley, F. L., "Attitude Estimation or Quaternion Estimation?" *Journal of Astronautical Sciences*, Vol. 52, Nos. 1–2, Jan.–June 2004, pp. 221–238.

[7] Kau, S., Kumar, K. S. P., and Granley, G. B., "Attitude Determination via Nonlinear Filtering," *IEEE Transactions on Aerospace and Electronic Systems*, Vol. AES-5, No. 6, 1969, pp. 906–911. doi:10.1109/TAES.1969.309965

[8] Bar-Itzhack, I. Y., and Idan, M., "Recursive Attitude Determination from Vector Observations: Euler Angle Estimation," *Journal of Guidance, Control, and Dynamics*, Vol. 10, No. 2, 1987, pp. 152–158. doi:10.2514/3.22911

[9] Idan, M., "Estimation of Rodrigues Parameters from Vector Observations," *IEEE Transactions on Aerospace and Electronic Systems*, Vol. 32, No. 2, 1996, pp. 578–586. doi:10.1109/7.489502

[10] Schaub, H., and Junkins, J. L., "Stereographic Orientation Parameters for Attitude Dynamics: A Generalization of the Rodrigues Parameters," *Journal of Astronautical Sciences*, Vol. 44, No. 1, 1996, pp. 1–19.

[11] Crassidis, J. L., and Markley, F. L., "Attitude Estimation Using Modified Rodrigues Parameters," *Proceedings of the Flight Mechanics/ Estimation Theory Symposium*, NASA Goddard Space Flight Center, Greenbelt, MD, 1996, pp. 71–83.

[12] Tsiotras, P., "Stabilization and Optimality Results for the Attitude Control Problem," *Journal of Guidance, Control, and Dynamics*, Vol. 19, No. 4, 1996, pp. 772–779. doi:10.2514/3.21698

[13] Schaub, H., and Junkins, J. L., "New Penalty Functions and Optimal Control Formulation for Spacecraft Attitude Control Problems," *Journal of Guidance, Control, and Dynamics*, Vol. 20, No. 3, 1997, pp. 428–434. doi:10.2514/2.4093

[14] Crassidis, J. L., and Markley, F. L., "Sliding Mode Control Using Modified Rodrigues Parameters," *Journal of Guidance, Control, and Dynamics*, Vol. 19, No. 6, 1996, pp. 1381–1383. doi:10.2514/3.21798

[15] Lee, D.-J., and Alfriend, K. T., "Additive Divided Difference Filtering for Real-Time Spacecraft Attitude Estimation Using Modified Rodrigues Parameters," *Journal of Astronautical Sciences*, Vol. 57, Nos. 1–2, 2009, pp. 93–111.

[16] Cheng, Y., and Crassidis, J. L., "Particle Filtering for Sequential Spacecraft Attitude Estimation," *Proceedings of the AIAA Guidance, Navigation, and Control Conference and Exhibit*, AIAA Paper 2004-5337, Aug. 2004.

[17] Jizheng, C., Jianping, Y., and Qun, F., "Flight Vehicle Attitude Determination Using the Modified Rodrigues Parameters," *Chinese Journal of Aeronautics*, Vol. 21, No. 5, 2008, pp. 433–440. doi:10.1016/S1000-9361(08)60056-4

[18] Schaub, H., and Junkins, J. L., *Analytical Mechanics of Space Systems*, AIAA Education Series, 2nd ed., AIAA, Reston, VA, Oct. 2009, pp. 79–142.

[19] Crassidis, J. L., and Junkins, J. L., *Optimal Estimation of Dynamic Systems*, CRC Press, Boca Raton, FL, 2004, pp. 419–433.

[20] Farrenkopf, R. L., "Analytic Steady-State Accuracy Solutions for Two Common Spacecraft Attitude Estimators," *Journal of Guidance, Control, and Dynamics*, Vol. 1, No. 4, 1978, pp. 282–284. doi:10.2514/3.55779

[21] Crassidis, J. L., and Junkins, J. L., *Optimal Estimation of Dynamic Systems*, CRC Press, Boca Raton, FL, 2004, pp. 243–342.